We are IntechOpen, the world's leading publisher of Open Access books Built by scientists, for scientists

4,800
Open access books available

122,000
International authors and editors

135M
Downloads

Our authors are among the

154
Countries delivered to

TOP 1%
most cited scientists

12.2%
Contributors from top 500 universities

CLARIVATE ANALYTICS BOOK CITATION INDEX INDEXED

WEB OF SCIENCE™

Selection of our books indexed in the Book Citation Index in Web of Science™ Core Collection (BKCI)

Interested in publishing with us?
Contact book.department@intechopen.com

Numbers displayed above are based on latest data collected.
For more information visit www.intechopen.com

5

POLICRYPS Composite Materials: Features and Applications

R. Caputo[1], L. De Sio[1], A. Veltri[1],
A. V. Sukhov[2], N. V. Tabiryan[3] and C. P. Umeton[1]
[1]LICRYL (Liquid Crystals Laboratory, IPCF-CNR), Center of Excellence (CEMIF.CAL) and Department of Physics, University of Calabria, Arcavacata di Rende, 87036 Cosenza,
[2]Institute for Problems in Mechanics, Russian Academy of Science, Moscow 119526,
[3]Beam Engineering for Advanced Measurements Company, Winter Park, Florida 32789,
[1]Italy
[2]Russia
[3]USA

1. Introduction

In recent decades, great attention has been devoted to the realization of electrically switchable holographic gratings in liquid crystalline composite materials. It has been shown, indeed, that devices based on holographic polymer dispersed liquid crystals (HPDLCs) are of low cost and can exhibit good diffraction efficiency (DE) [Margerum et al, 1992; Sutherland et al, 1996]. However, application oriented utilization of these devices is limited, in general, by their strong scattering of light, due to the circumstance that the droplet size of the nematic liquid crystal (NLC) component inside the polymer matrix is comparable to the wavelength of the impinging light. In this framework, we have recently proposed a new kind of holographic grating called POLICRYPS, made of polymer slices alternated to films of regularly aligned NLC. These structures do not present those optical inhomogeneities that are due to the presence of NLC droplets in usual HPDLC samples [Sutherland et al, 1994], and can therefore exhibit good optical characteristics, with values of the diffraction efficiency as high as 98%.

This chapter is devoted to give an overview of the POLICRYPS as a composite material, along with a description of its main applications. After a short presentation of the structure, in terms of its fabrication process, we present the POLICRYPS as the device it was initially designed for: a switchable diffraction grating. We also demonstrate that, by suitably choosing the sample thickness and geometrical parameters, a POLICRYPS put perpendicular to the impinging light can behave as a switchable optical phase modulator, where the retardation between ordinary and extraordinary waves can undergo a fine electrical regulation. It is very interesting to show how by adding dye materials to the initial chemical mixture, necessary for obtaining POLICRYPS, can change the way we control its functionalities. In this case, such control can be obtained by using a laser beam of the right colour and power. This fact allows the realization of completely new applications like an optically controlled tunable beam splitter.

New intriguing sceneries open when using different materials to realize POLICRYPS. In particular, if a dye-doped cholesteric liquid crystal (instead of a nematic liquid crystal) is used, the POLICRYPS polymeric channels become mirrorless optical cavities where a distributed feedback (DFB) lasing effect (with a very low threshold) can be obtained. Another challenging opportunity is offered in case a tiny concentration of metallic nanoparticles is included in the initial POLICRYPS mixture. By doing so, we obtain a new device whose frequency spectrum is dependent on the probe light polarization. This last possibility is still in progress and is oriented to the realization of a POLICRYPS structure with meta-material properties.

2. The POLICRYPS structure

The morphology of the POLICRYPS is quite different from the HPDLC one. Optical microscope and scanning electronic microscope (SEM) investigations have shown that the structure consists of rigid slices of almost pure polymer alternated to films of almost pure NLC. The polymeric slices are well glued to two glasses that confine and contain the POLICRYPS. These slices represent a rigid frame that, somehow, 'stabilizes' the NLC component and, therefore, the whole sample. Separation interfaces between polymer slices and NLC films are quite regular and sharp; furthermore, there is convincing evidence that, at these interfaces, the NLC director is everywhere perpendicular to them, thus inducing a good, uniform alignment of the director in the whole NLC film standing between two polymeric slices. This circumstance represents one of the main features that determine the overall characteristics of the whole structure. The uniform and regular alignment of the director in the NLC films of the structure determines the main optical and electro-optical properties of the POLICRYPS. From the optical point of view, losses due to the scattering of the visible light (which is eventually brought to impinge onto the POLICRYPS) are reduced to less than 2%, thanks to the absence of droplets, which exist in HPDLC samples, with an average size comparable to the light wavelength and an arbitrary director alignment. From an electro-optical point of view, the fact that the NLC molecules are confined (and well aligned) in a uniform film, rather than in a small droplet, allows a suitably oriented electric field of the order of a few V/μm to uniformly 'reorient' the NLC director in a millisecond timescale. Afterwards, by suitably choosing the values of the refractive index of the polymer and the ordinary/extraordinary refractive index of the NLC, this director reorientation can be exploited to vary the spatial modulation of the refractive index of the POLICRYPS.

2.1 Fabrication process and set-up

The standard procedure that enables the realization of a good POLICRYPS structure exploits the high diffusivity of NLC molecules in the isotropic state, which avoids the formation and separation of the nematic phase (as NLC droplets) during the curing process [Caputo et al, 2000, 2004, 2007]. The main fabrication steps can be illustrated as follows. By means of a hot stage, a syrup of NLC, monomer and photo-initiator is heated up to a temperature which is above the nematic–isotropic transition point of the NLC component; the sample is then 'cured' with the interference pattern of a UV radiation. After the curing process has come to an end, the sample is brought below the isotropic–nematic transition point by means of a controlled, very slow, linear cooling down to room temperature. The experimental set-up exploits an active system for suppression of vibrations [De Sio et al, 2006, 2008a] and is presented in Fig. 1. An Ar-ion laser is the source of a single-mode radiation at the

wavelength λ_B = 351 nm. The beam is broadened up to a diameter of about 25 mm by the beam expander BE, and divided into two beams of almost equal intensity by the beam splitter BS. These two beams overlap and give rise to the 'curing' interference pattern at the entrance plane of the sample cell S, whose temperature is controlled by the hot stage. Depending on the required nano/microscale dimensions of the structure, the spatial period of the interference pattern can be varied in the range Λ = 0.2–15 μm by adjusting the total interference angle $2\theta_{cur}$. A commercial, metal-coated, reflective diffraction grating (Edmund Optics) placed above the sample is used as a test element for the interferometric monitoring of vibrations. Part of each of the curing beams is reflected and diffracted by this grating. The set-up is adjusted to make the reflected part of one beam spatially coincident with the diffracted part of the second one. These two radiations are wave coupled by the test grating and their interference pattern is detected by an additional photodiode PD3. The signal of this photodiode is sent to a computerized active feedback system, which exploits a software that is based on a proportional–integral–derivative (PID) protocol; this drives a mirror-holder whose position can be controlled by a piezoelectric mechanism, used in feedback configuration. This control system has proved to be able to continuously compensate for changes in the optical path length due to vibrations as well as variations in environmental conditions such as room pressure, temperature or humidity; residual fluctuations are of the order of 6–7 nm, which correspond to the sensitivity of the piezo-system used.

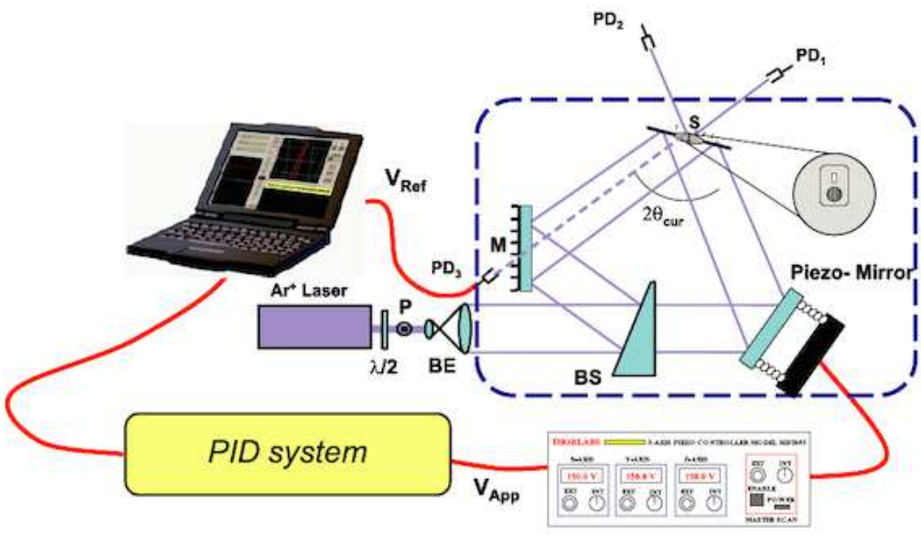

Fig. 1. Optical holographic set-up for UV curing of gratings with stability check. P, polarizer; λ/2, half-wave plate; BE, beam expander; BS, beam splitter; $2\theta_{cur}$, total curing angle; M, mirrors; S, sample; PD1, first beam photo-detector; PD2, second beam photo-detector; PD3, diffracted/reflected beam photo-detector. In the insertion the reference grating is shown (put immediately below the sample area) which enables the stability check

3. The POLICRYPS grating/phase modulator

3.1 POLICRYPS as a high quality, switchable, diffraction grating

The basic device that can be realized by using electrically switchable holographic gratings in liquid crystalline composite materials is an electro-optical switch [Sutherland et al, 1994].

Such a device should, in principle, completely diffract or transmit an impinging light beam, depending on the application of an external voltage (Fig. 2).

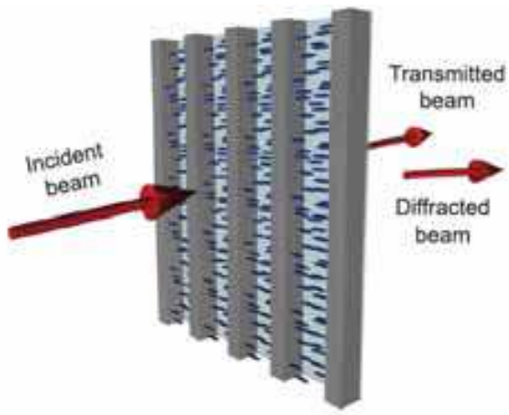

Fig. 2. Sketch of a POLICRYPS grating in transmission configuration

PDLCs have been actively utilized in the past in order to realize working prototypes of this kind of device; unfortunately, they still show issues that affect their performances. One of the main reasons that brought us to design POLICRYPS systems was the possibility of overcoming most of these issues. In the following, we report the results of an experimental comparison between an HPDLC and a POLICRYPS grating, in order to put into evidence how microscopic features of the structure can influence the overall performance of the macroscopic device. We have realized a standard HPDLC and a POLICRYPS grating, both with a fringe spacing Λ=1.5 μm. Sample cells, 16 μm thick, made with indium tin oxide (ITO)-coated glass slabs, were filled with the same initial chemical syrup. This was prepared by diluting the NLC 5CB (Merck, ≈30 wt%) in the prepolymer system Norland Optical Adhesive NOA-61. The POLICRYPS grating was cured by a total UV intensity of 11 mW/cm², acting on the sample for τ≈1000 s at high temperature (e.g. above the nematic–isotropic transition point of the 5CB liquid crystal), these being the optimal conditions for achieving a high diffraction efficiency and a morphology of good quality [Caputo et al, 2001]. Almost the same UV intensity and curing time proved also to be adequate for the realization of the PDLC grating, but in this case the sample was cured at room temperature. In order to explore the performances of both gratings, we used a weak (P≈1mW) He–Ne laser radiation (λ_R=633 nm), with its angle of incidence adjusted for satisfying the Bragg condition for the first-order diffracted beam. With the aim of performing a comparison in the same experimental conditions, before starting the curing process of each sample, we measured the intensity I_{in} of the impinging probe beam (before the sample) and the transmitted intensity I_{tr}. Then, once the curing process had been completed and the UV light switched off, we measured both the intensity I_0 of the zero-order (direct transmitted) probe beam and the intensity I_1 of the first-order diffracted probe beam. In this way we were able to calculate the zero-order transmittivity $T_0=I_0/I_{in}$, the first-order transmittivity $T_1=I_1/I_{in}$, the total transmittivity $T_{tot}=T_0+T_1$ and the first-order diffraction efficiency, which is usually calculated as $\eta_1=I_1/I_{tr}$. During all the experiments, the intensity of the probe beam was maintained at a fixed value (the value of the initial impinging intensity before the curing process started). We measured the first-order diffraction efficiency at room temperature

both for POLICRYPS and HPDLC gratings, obtaining $\eta^1_{POLICRYPS}$ = 88% and η^1_{HPDLC} = 41.2%. We stress that the value of $\eta^1_{POLICRYPS}$ is not the highest that we can get since, by using other POLICRYPS gratings (not involved in comparisons with HPDLC ones), we have obtained $\eta^1_{POLICRYPS}$ values as high as 98%. The electro-optic response of the two gratings was investigated by exploiting a low frequency (500 Hz) square-wave voltage, and results are reported in Fig.3.

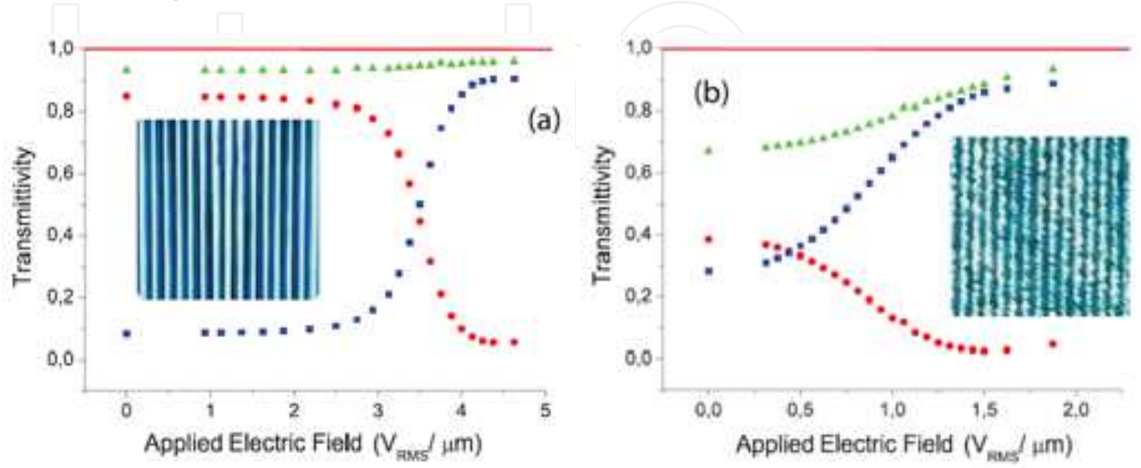

Fig. 3. Dependence on applied voltage of the zero-order transmittivity T_0 (squares), first-order transmittivity T_1 (circles) and total transmittivity T_{tot} (triangles) for (a) a POLICRYPS grating and (b) an HPDLC grating at room temperature. Error bars are of the order of the dot size. The pictures in the inset show respectively a typical POLICRYPS and HPDLC grating morphology observed under a polarizing optical microscope

Fig. 3a represents the switching curve of the POLICRYPS grating: the behaviour of the first-order transmittivity T_1 (circles), zero-order transmittivity T_0 (squares) and total transmittivity T_{tot} (triangles) is reported versus the root mean square applied electric field.

	$\tau_{fall}\,(\mathrm{ms})$	$\tau_{rise}\,(\mathrm{ms})$
POLICRYPS	1.12 ± 0.03	0.88 ± 0.03
HPDLC	10.53 ± 0,18	1.36 ± 0.04

Table 1. Measured values of the switching times for a POLICRYPS and an HPDLC grating obtained from the same initial mixture

It is worth noting that T_{tot} is only slightly lower than 1 and remains approximately the same for all values of the applied field; this indicates that the grating exhibits negligible scattering losses. The situation is quite different for the HPDLC grating (Fig. 3b): the total transmittivity is well below 1 and increases as the applied field increases. We also note that the switching efficiency $h_{sw} \equiv \frac{T^1_{on} - T^1_{off}}{T^1_{on}}$, where T^1_{on} and T^1_{off} are the first-order transmittivities in the switch-on and switch-off condition respectively, is almost the same (93.3%) for both gratings. Where the switching fields are concerned, the first diffracted beam is almost completely switched off by a field of about 1.5V/μm applied to the HPDLC grating, while a value of about 4.3V/μm is needed to obtain the same effect in the

POLICRYPS one. This particular difference can be due to the average size of NLC droplets in the HPDLC; evidently, this size is large enough to enable low switching fields. This is confirmed by the values of the switching times shown in table 1: both the rise and fall times of the HPDLC grating are longer than those of the POLICRYPS; this suggests a very large average size of PDLC droplets. Here, we stress that the electro-optic behaviour shown in Fig. 3a, and its noticeable difference with the one of Fig. 3b, represents the best evidence of the good performances of POLICRYPS gratings; indeed, people working with HPDLCs of nanosized droplets also find for these materials behaviours that are comparable to the one shown in Fig. 3a, but for values of the switching fields which are about four-fold higher [Lucchetta et al, 2003].

3.2 POLICRYPS as an optical phase modulator

The preferential orientation and the good alignment assumed by the molecular director **n** of the LC material within a POLICRYPS structure recently suggested a possible use of these systems as switchable phase modulators [De Sio et al, 2008b]. Examples of such devices are already present in literature. A basic embodiment is obtained by enclosing a NLC with a positive dielectric anisotropy in a cell made of two ITO-coated glasses, treated to give a planar alignment to the NLC director. Since the liquid crystal is birefringent, light with wavelength λ, propagating through the structure, is separated into an ordinary and an extraordinary component. If L is the thickness of the sample and Δn_{LC} indicates its birefringence, the phase difference δ_{LC} between these two waves, measured at the exit of the sample, depends on the value of Δn_{LC}: $\delta_{LC}=2\pi L\Delta n_{LC}/\lambda$. By applying an external electric field **E** with direction perpendicular to the glass slabs of the cell, **n** tends to reorient along the same direction as **E**, thus producing a change in the phase difference. However, this simple device presents some drawbacks. The orientation of **n** is, indeed, sensitive to temperature changes [de Gennes, 1993]. This can represent a serious limit for an eventual device when the power of the impinging radiation is high. Moreover, the switching times of such devices are usually quite long (2–8 ms), thus limiting the field of possible applications. In order to overcome the above-mentioned problems, the NLC layer is often stabilized by means of polymeric chains [Wu et al, 2004]; their presence improves the response times of the device but, unfortunately, drastically increases the operating voltages (due, probably, to the torque exerted by the polymer on the nematic director). Moreover, due to the irregularity of morphology induced by the presence of polymeric chains, visible light is strongly scattered. Therefore, these systems are suitable only for wavelengths in the infrared range. Several features of POLICRYPS structures make them an attractive alternative to the discussed system. First of all, they exhibit limited scattering losses when illuminated by visible light. Second, the polymer slices confine and stabilize the NLC molecules, thus also influencing their alignment, and third, POLICRYPS structures can be driven by low voltages exhibiting short switching times. We expect that the better the alignment of the NLC director in the nematic layer of the POLICRYPS, the higher the value of Δn_{LC}; then, the phase retardation introduced by the grating will depend on the angle that the polarization vector of the impinging light forms with the nematic director within the LC layers Fig. 4.

It is important to underline that, because of the diffractive nature of a POLICRYPS structure, the light impinging on the device will not only experience a phase modulation but will also undergo a dichroic absorption as explained in [Caputo et al, 2010]. This double behaviour can be taken into account by considering the POLICRYPS, in terms of the Jones matrix formalism, as both a retardation plate and a dichroic absorber. This is done by multiplying the Jones Matrix of the generic phase retarder by a new matrix L given by:

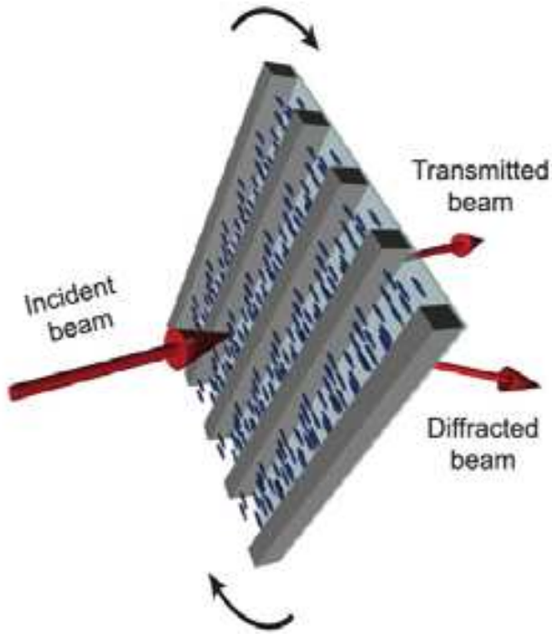

Fig. 4. Sketch of a POLICRYPS grating in transmission configuration used as a phase modulator

$$L = \begin{pmatrix} H & 0 \\ 0 & V \end{pmatrix} \tag{1}$$

where H and V parameter values depend on the considered material and can reflect a broad range of situations. The POLICRYPS used for experiments as a phase modulator has a thickness L=3.03μm and a fringe spacing Λ=1.22μm. In order to check the phase retardation properties of this structure, we used the experimental set-up reported in Fig. 5. The POLICRYPS is put between a polarizer P and an analyzer A, with its optical axis oriented at an angle $\theta=\pi/4$ with respect to the first polarizer; in this position, the field components have the same amplitude ($E_{||}=E_{\perp}$) and the sample introduces the maximum retardation.

During experiments, the position of the sample remains fixed while the analyzer is rotated (in steps of 10°) around the axis of propagation of the probe light (z axis in Fig. 5). We define β as the angle between directions of analyzer and incident polarization (therefore β=0 when the analyzer A is parallel to the polarizer P). If we indicate with I_{inc} the intensity of the impinging beam, by means of eqs (2) and (3) (derived in [Caputo et al, 2010]), it is possible to calculate the complex electric field $\tilde{E}_{out}(\beta)$ and hence the intensity $I_{out}(\beta)$ of light transmitted by the analyzer A in our experimental geometry.

$$\tilde{E}_{out}(\beta) = \frac{\sqrt{2}}{2}\sqrt{I_{inc}} \begin{pmatrix} -He^{i\frac{\delta}{2}}\sin^2\beta - Ve^{-i\frac{\delta}{2}}\sin\beta\cos\beta \\ He^{i\frac{\delta}{2}}\sin\beta\cos\beta + Ve^{i\frac{\delta}{2}}\cos^2\beta \end{pmatrix} \tag{2}$$

$$I_{out}(\beta) = \tilde{E}_{out}(\beta)\cdot\tilde{E}^{*}_{out}(\beta) = \frac{I_{inc}}{2}\left[H^2\sin^2\beta + V^2\cos^2\beta + HV\sin 2\beta\cos\delta\right] \tag{3}$$

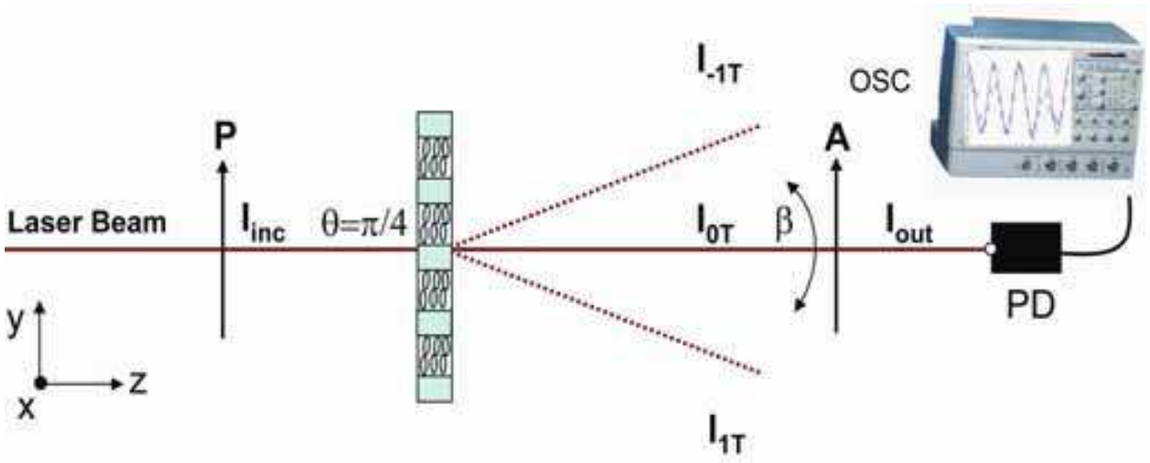

Fig. 5. Experimental geometry utilized for measuring the intensity transmitted by the system composed of a birefringent/dichroic sample put between two polarizers. P polarizer, A analyzer, I_{inc} total incident intensity, I_{out} output intensity, I_{0T} and $I_{\pm 1T}$ zeroth and first order transmitted intensities, respectively. θ is the angle between the light polarization direction (y axis) and the grating optical axis (laying in the xy plane), PD Photo-detector, OSC oscilloscope. The probe beam is from a He-Ne laser at the wavelength λ=632.8 nm. S is the POLICRYPS sample

Parameters H and V are given by:

$$H = \sqrt{\frac{2I_{out}\left(\beta = \pi/2\right)}{I_{inc}}} \tag{4}$$

$$V = \sqrt{\frac{2I_{out}\left(\beta = 0\right)}{I_{inc}}} \tag{5}$$

While the phase retardation δ introduced by the sample can be calculated as:

$$\cos\delta = \frac{1}{HV}\left[\frac{2I_{out}\left(\beta = \pi/4\right)}{I_{inc}} - \frac{H^2 + V^2}{2}\right] \tag{6}$$

By substituting obtained data in eqs. (4), (5) and (6), we obtain: H=0.727, V=0.406 and δ=1.26rad. In Fig. 6, the experimental value of I_{out} as a function of the angle β (crosses) is compared with the theoretical behavior predicted by eq. 3 (solid line).

The different values of H and V show that, even at normal incidence, the diffraction efficiency of the POLICRYPS grating is significant. As for the birefringence of the structure, the obtained value of δ yields Δn=0.042. By considering that the periodicity of the grating is much larger than the probe wavelength we can exclude that this considerably high value is due to form birefringence and hence to the geometrical features of the grating. We are confident, instead, that this value indicates that the stabilizing and confining action exerted by polymer slices on the NLC molecules has a direct influence on their alignment.

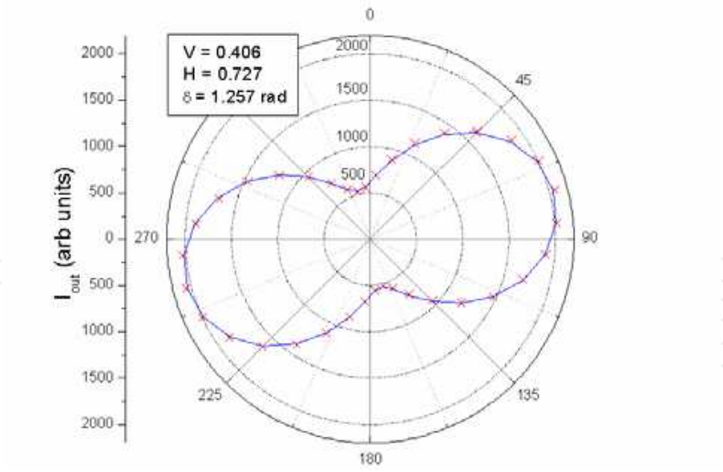

Fig. 6. Behaviour of the intensity transmitted by the analyzer put after a POLICRYPS grating as a function of the angle β between the electric field of the impinging wave and the axis of the analyzer itself. Two segments in the graph evidence output intensity values for the analyzer positions β=0 and β=π/2 respectively

3.2.1 Tunability of the phase retardation

In order to verify the functionalities of POLICRYPS as a tunable phase retarder, we prepared another sample whose thickness had a wedge shaped profile [Caputo et al, 2011a]. As discussed above, by applying an external electric field we can change the birefringence and hence the phase retardation introduced by the structure. However, the phase retardation also depends on the thickness of the layer in which the light propagates. This explains the choice of a wedge shaped cell: by combining the application of the electric field and the possibility to shift the sample to get the desired thickness, it is possible to achieve a very fine tunability for our device. The realized wedge-shaped structure has a thickness varying in the interval (3.00÷5.00 μm) and has been experimentally characterized by means of the setup shown in Fig. 5. The check of the electro-optical tunability of the sample birefringence, has been performed by probing the fabricated sample in the area corresponding to a thickness L=4.35μm. This and other thickness values have been measured before filling the cell by means of an Agilent spectrophotometer and considering the cell as a Fabry-Perot etalon. The applied electric field is a bipolar square wave with frequency ν=1 kHz and a peak-to-peak amplitude varying in the interval (0÷9 Volts/μm). Measurements of the intensity $I_{out}(\beta)$ of light transmitted by the analyzer A have been performed by changing β in the interval 0≤β≤2π, for different values of the applied electric field. Obtained results show that the application of an electric field produces a tuning action of the phase retardation from 1.64rad to 1.07 rad. In each curve of Fig. 7, dots represent experimental values whereas solid lines indicate theoretical predictions; it is evident that the agreement is very good. The plot of both the birefringence value Δn (red dots) and the phase retardation δ (blue dots) of the structure, calculated considering a thickness L=4.35μm, are reported in Fig. 8 as a function of the applied electric field. Phase retardation variations yield, in this case (λ=632.8nm), to a birefringence value varying in the interval (0.024÷0.038). The phase retardation/birefringence properties of our POLICRYPS structure can be also varied by shifting the probed area of the sample along the wedge direction. Several positions have been probed. Experimental results and corresponding theoretical curves are shown in Fig. 9.

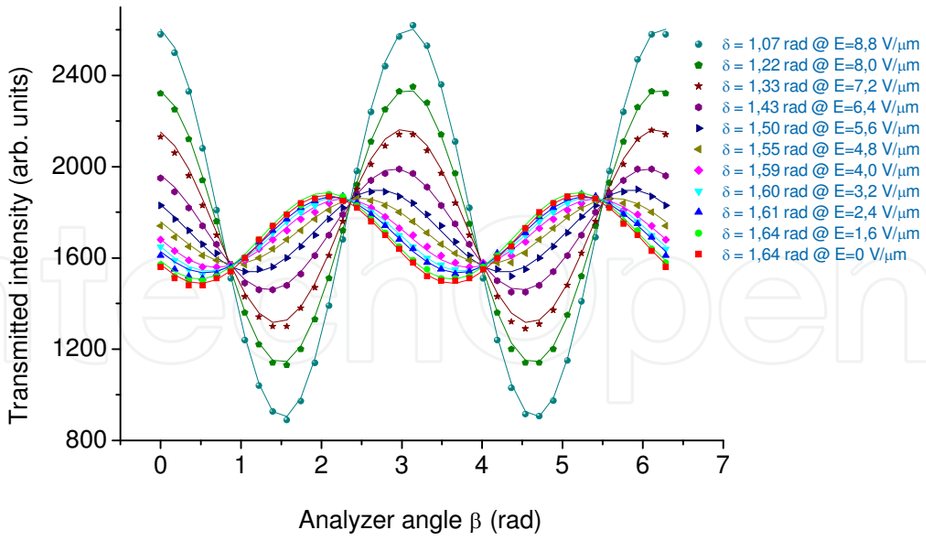

Fig. 7. Behavior of the intensity transmitted by the analyzer put after the POLICRYPS grating obtained by changing the amplitude of the applied electric field. For each amplitude, the output intensity has been measured by varying β between 0 and 2π. Solid lines are theoretical fits while dots represent experimental data. Experimental errors are of the order of the dot size

Also in this case, results confirm the possibility of tuning the phase retardation at will by just probing the sample in the position where it has the right thickness.The thickness value L=4.10μm corresponds to a phase retardation δ=1.55rad (orange curve in Fig. 9) which is close to the condition of quarter wave plate for the He-Ne laser wavelength. This curve is almost constant for every β angle, as expected for this particular value of the phase retardation.

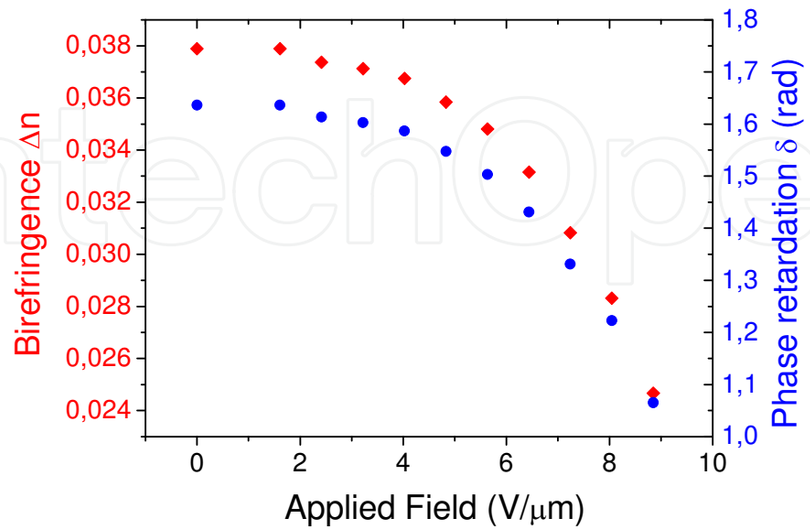

Fig. 8. Plot of birefringence Δn (red dots) and phase retardation δ (blue dots) of the POLICRYPS structure versus the amplitude of the applied electric field

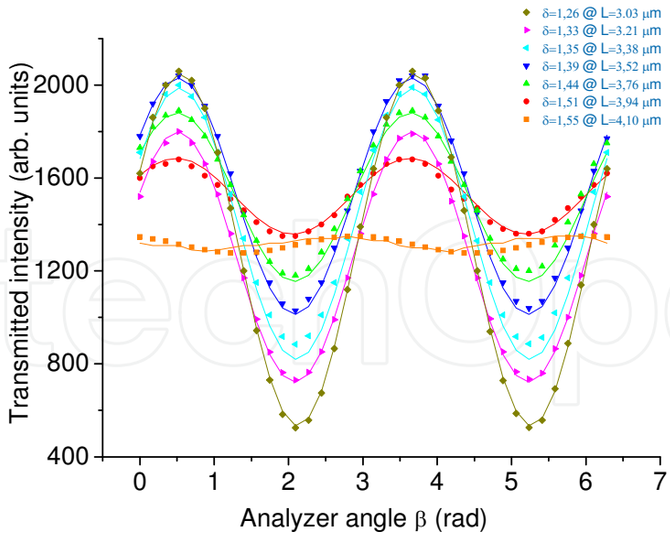

Fig. 9. Behavior of the intensity transmitted by the analyzer put after a POLICRYPS grating obtained by shifting the sample along the wedge direction and probing it in areas with different thickness. For each thickness, the output intensity has been measured by varying β between 0 and 2π. Solid lines are theoretical fits while dots represent experimental data. Experimental errors are of the order of the dot size

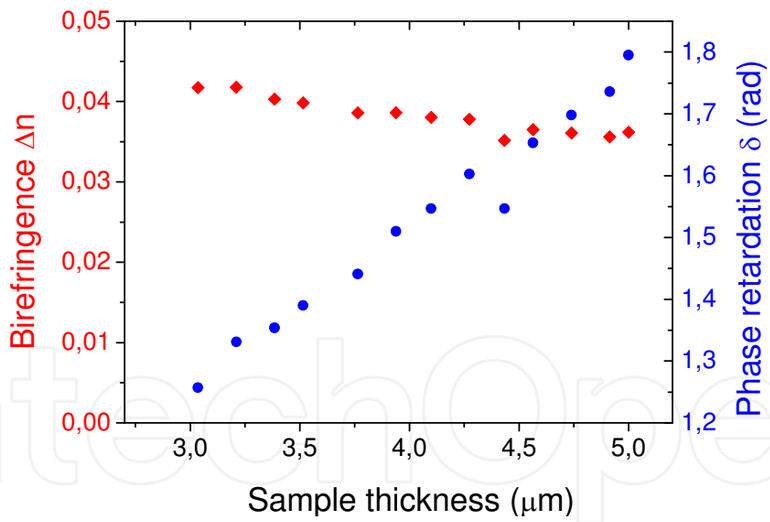

Fig. 10. Plot of birefringence Δn (red dots) and phase retardation δ (blue dots) of the POLICRYPS structure measured by shifting the sample along the wedge direction and probing it in areas of different cell thickness

This result confirms the possibility of finely tuning the phase retardation introduced by the structure by playing both with the amplitude of the applied electric field and the position of the sample for finding the area corresponding to the optimal thickness.
Birefringence and corresponding phase retardation values, measured by shifting the sample along the wedge direction, are reported in Fig. 10. We can notice that, by increasing the thickness L in the interval (3.0÷5.0μm), Δn remains almost constant, as expected if we

consider that the POLICRYPS grating exhibits a quite homogeneous morphology. On the contrary, the phase retardation δ shows a linear increase with values varying in the interval (1.25÷1.80 rad).

4. Photoresponsive POLICRYPS structures

As discussed above, a fundamental advantage provided by holographic structures containing liquid crystal materials is the possibility of tuning their optical properties by applying external electric or thermal fields. Some years ago, Tondiglia et al. have proposed another fascinating possibility: the use of light for switching the optical properties of gratings [Bunning et al, 2000]. Indeed, azobenzene liquid crystals enable to access, optically and isothermally, a nematic to isotropic (NI) transition that changes the refractive index of the liquid crystal films, thus modifying the refractive index modulation of the whole structure. The exploited mechanism is that, upon UV (λ=360 nm) irradiation, azo-LC molecules undergo a conformational change (from rodlike trans to cis) which drives the LC through an isothermal NI phase transition; this process can be driven in the reverse direction by converting the cis-azobenzene moieties back to their rodlike *trans* state via exposure to a radiation of a suitable wavelength [Tsutsumi & Ikeda, 1995]. The decision to adopt these materials in the initial POLICRYPS mixture brought to the realization of the so-called azo-POLICRYPS: optically controlled POLICRYPS structures. Samples have been realized by means of the typical setup for POLICRYPS fabrication (reported in Fig. 11). Preliminary attempts, performed on different sample cells, have shown that the best performances are exhibited by the one of L=11.4μm thickness, with a grating pitch Λ=1.6μm, this value being such that the highest diffraction efficiency is obtained with the actual cell thickness. Samples have been prepared by using the following mixture: 25 wt % of NLC (E7 by Merck), 5 wt % of azo-LC (1005 by BEAM Co.), and 70 wt % of monomer (NOA61 by Norland). A qualitative characterization, made with an optical microscope, shows that this azo-POLICRYPS exhibits a stable structure, made of alternated layers of pure polymer and pure LC, with the apparent absence of PDLC droplets (inset of Fig. 11).

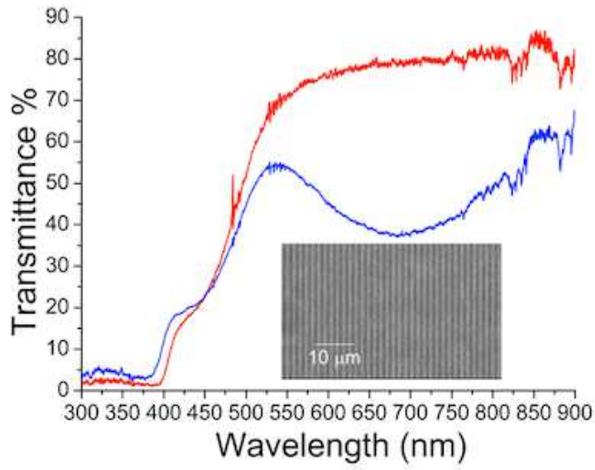

Fig. 11. Transmission spectra of both the uncured mixture (red curve) and the realized grating (blue curve). Inset: photo of a POLICRYPS grating taken with a 20x objective equipped Olympus microscope

Transmission spectra reported in Fig. 11 have been obtained with the aid of a fiber optic spectrometer, using light beams of arbitrary polarization at normal incidence. The mixture exhibits a high absorption in the λ=300–400 nm range, while the grating gives rise to a relative minimum in the transmission around λ=650 nm.

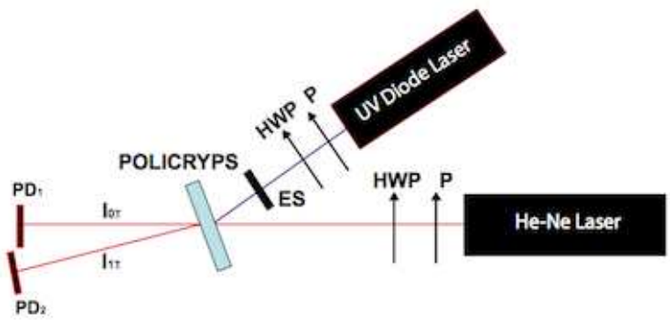

Fig. 12. Experimental setup for the observation of all-optical processes in azo-POLICRYPS. $PD_{1,2}$: photodetectors; HWP: half-wave plate; P: polarizer; ES: electronic shutter

Thus, the setup utilized for the characterization of the sample (Fig. 12) makes use of an UV diode pump laser emitting at λ=409 nm (in the high absorption range of the mixture spectrum) and a He–Ne probe beam of λ=633 nm (in the range that is of high efficiency for the grating); this beam impinges at the Bragg angle θ=11.5°. For experimental simplicity, we have used an unfocused pump beam with a power of only 4.4 mW, which exhibits an oval shape on the sample of about 2-3 mm^2. Fig. 13 shows that a pump irradiation of duration τ=20 s, operated by opening the electronic shutter (ES), reduces the diffraction efficiency of the azo-POLICRYPS grating to less than 75% of its initial value in a time of a few seconds; a slow increase toward the initial value is then observed when the shutter closes the pump beam.

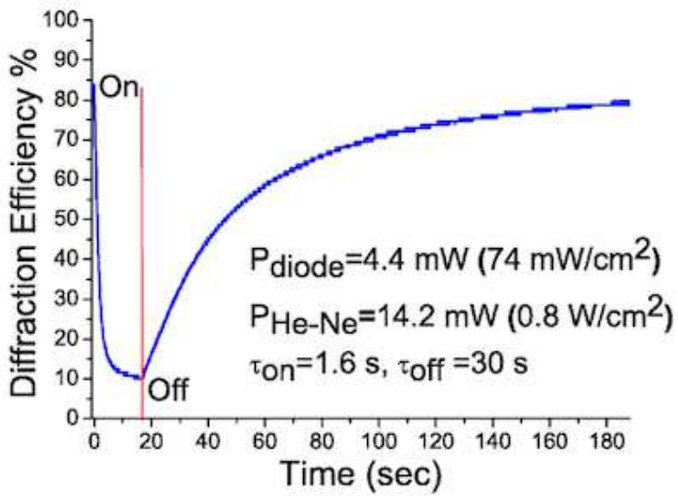

Fig. 13. Dynamics of the diffraction efficiency of the probe first order diffracted beam. The diffraction efficiency of the grating is de- fined as the diffracted intensity divided by the sum of the diffracted and transmitted intensities

We have investigated this dynamics by varying the pump power from 0.1 mW to 14.6 mW, while the probe power is kept constant: (inset of Fig. 14).

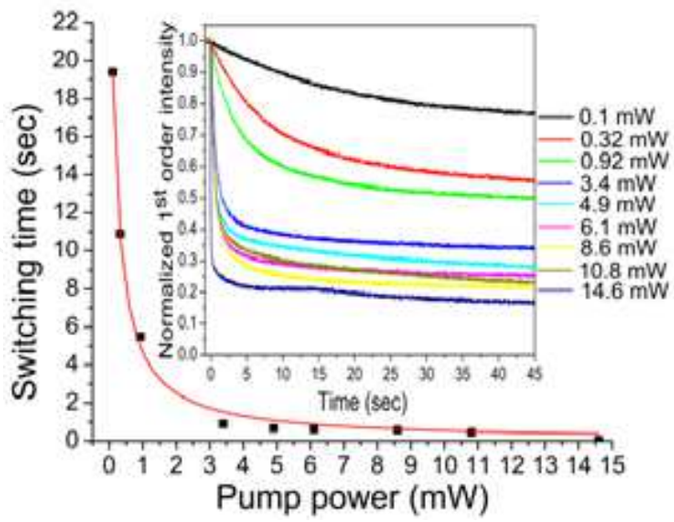

Fig. 14. Response time of the azo-POLICRYPS grating vs the power of the pump beam; the error bar is of the order of the square dimension. Diffraction efficiency values in the inset are normalized to the initial ones

The switching time (sw) of each curve is reported in Fig. 14 as a function of the impinging pump power P: when this power exceeds a minimum value $P_{min}\cong 0.1$ mW (below which the effect is very small and it is almost impossible to get a good signal), data are well fitted by the negative exponential red curve,

$$\tau_{sw} = \tau_0 e^{-(P-P_{\min})/P_0} \tag{7}$$

where τ_0=19.4 s and P_0=1.8 mW; this behavior can be explained by assuming the rate of concentration of photoisomerized azo-LC molecules proportional to the impinging intensity.Taking into account that in the actual experiment the pump beam is not focused, we foresee that much shorter switching-off times can be achieved in systems irradiated by a focused beam, where a high power density is obtained with power levels even lower than the actual ones.

4.1 azo-POLICRYPS as an optically controlled beam-splitter

The possibility to realize an optically controlled POLICRYPS structure is of particular interest for applications, since fast light responsive devices represent an innovative way to realize an on-chip technology. A fundamental element of an optical set-up is the beam-splitter. This element splits an incident light beam into two or more beams, which may or may not have the same intensity. These devices are usually passive in the sense that the intensity of the splitted beams is fixed or it can be eventually varied by changing the angle of incidence of the light impinging on the device. POLICRYPS diffraction grating can combine the capability of "dividing" beams (typical of periodic structures) with the effects of an adjustable birefringence, typical of nematic liquid crystals, which influences the intensities of the diffracted beams.

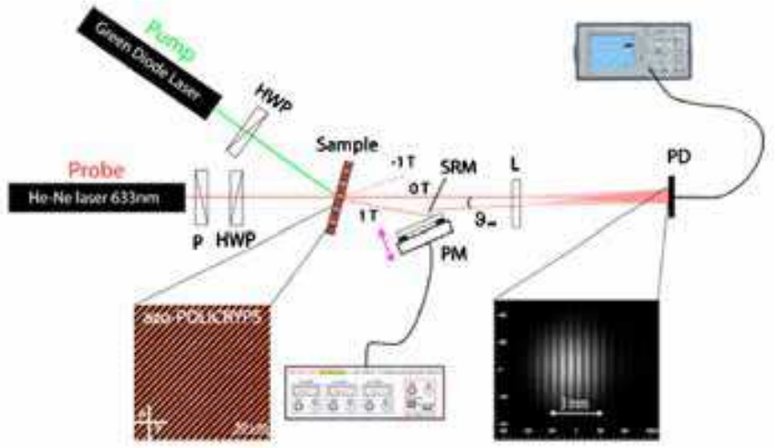

Fig. 15. All-optical OBS and interferometer setup: P, polarizer; HWP, half-wave plate; SRM, semireflective mirror; θ_{int}, interference angle; PM, piezomirror; PD, photodetector; L, lens

By using an azo-POLICRYPS as an optical beam splitter (OBS) it is possible to obtain a tunable optical element, where we can choose, at will (turning a knob), the portion of initial intensity which remains to the transmitted beam and the amount which is transferred to the splitted (diffracted) one. For the experiment, we have fabricated an azo-POLICRYPS structure whose geometrical parameters are L=6.95μm in thickness and Λ=1.57 μm in fringe spacing; according to Kogelnik's theory, [Kogelnik, 1969] this grating operates in the Bragg regime with a characteristic parameter $\rho=\Lambda^2/\lambda L=0.56$ at $\lambda=0.633$ nm. The experimental setup utilized to exploit the azo-POLICRYPS as a finely adjustable, optically controlled OBS is reported in Fig. 15. The impinging probe light is split into two beams (the transmitted and the diffracted orders, 0T and 1T respectively) by the azo-POLICRYPS grating. These are recombined in Mach–Zehnder interferometer geometry; this part of the setup is actually used to monitor the functionality of the OBS. The diffraction efficiency change of the azo-POLICRYPS is driven by an external pump source green diode laser. On application of the pump laser, the index contrast of the grating vanishes and the structure becomes transparent to the impinging probe light. Fig. 16a shows the evident change in the diffraction efficiency induced by switching ON the pump green light.

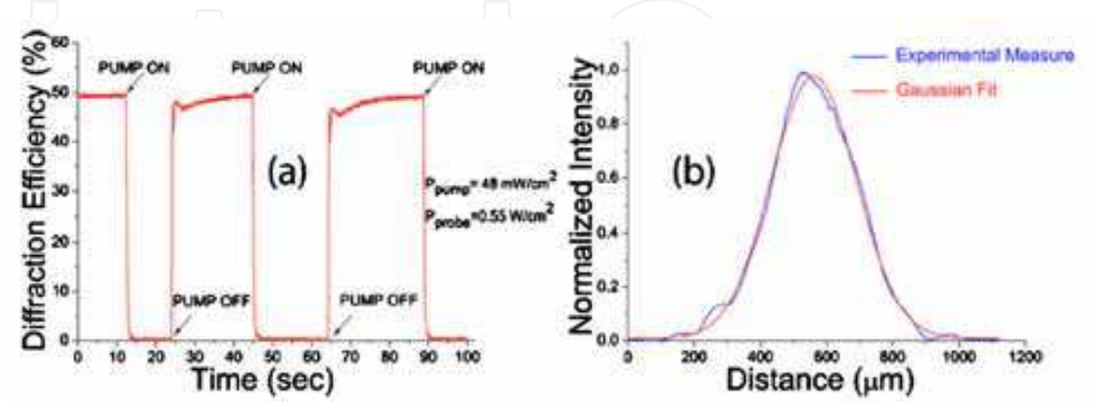

Fig. 16. (a) Reversible and repeatable changes of the azo-POLICRYPS diffraction efficiency induced by a pump green light. Power density values are reported in the figure; (b) Typical intensity profile of the transmitted intensity trough the structure

The switching response of the azo-POLICRYPS OBS is detected by using a sequence of ON-OFF pump beam irradiance P_{pump}=48 mW/cm² while the intensity of the probe red beam is kept ON at all times P_{probe}=0.55 W/cm².
As for the quality of the transmitted (0T) and diffracted (1T) beams outgoing from our OBS, we have detected their transverse intensity profiles with a charge-coupled device CCD camera for different increasing values of the incident probe power; we had the evidence that the grating does not modify the typical Gaussian shape of both beams, which remains almost unchanged for any value of the impinging probe power density in the range 0.1 to 0.7 W/cm²; Fig. 16b shows the Gaussian profile of the transmitted beam detected for the value P_{probe}=0.7 W/cm². The ratio $R=I_{1T}/I_{0T}$ of the intensities of 1T and 0T beams is related to the diffraction efficiency of the azo-POLICRYPS through the equation

$$\eta = \frac{I_{1T}}{I_{0T} + I_{1T}} = \frac{R}{1+R} \tag{8}$$

For the aim of the actual work, the polarization of the probe beam and its incident angle have been adjusted to obtain a maximum diffraction efficiency value max=50%, that is to say R_{max}=1, when the pump beam is off [De Sio et al, 2010]. In order to characterize and exploit the azo-POLICRYPS as a variable OBS, we have used the interferometer setup reported in Fig. 15. The interference pattern reported in the dark insets of Fig. 15 produced by overlapping 0T and 1T beams is monitored by means of the detector PD, which is provided of a small aperture 500 μm on top of the active area. The pattern periodicity can be easily controlled by varying the orientation of the semireflecting mirror, thus the angle θ_{int}. In our experiment, θ_{int} was relatively small 0.04°, and the scale is reported in the same dark inset of Fig. 15. The fringe visibility, defined as $\nu=(I_{max}-I_{min})/(I_{max}+I_{min})$, (where I_{max} and I_{min} are the measured maximum and minimum intensity values of the interference pattern) strongly depends on R. Indeed, for our geometry, it is easy to see that

$$\nu = \frac{2\left(I_{0T}I_{1T}\right)^{1/2}}{I_{0T}+I_{1T}}|\gamma| = \frac{2R^{1/2}}{1+R}|\gamma| \tag{9}$$

Here, γ (the degree of coherence of the two beams [Yariv, 1989] is related to the difference Δl of the optical path lengths of the two beams and to the coherence length lc of the probe laser beam, which in our case is of the order of 10 cm (HRP050 Thorlabs). We can assume that Δl does not exceed few micrometer even when the piezomirror (PM) is shifted back and forward of few micrometer, therefore $|\gamma|=(1-\Delta l/l_c)\approx 1$. Relating η to R by the equation $R=\eta/(1-\eta)$ and substituting it into eq. (9) we obtain:

$$\nu = 2\left(\frac{\eta}{1-\eta}\right)^{1/2} \tag{10}$$

Since in our azo-POLICRYPS grating η varies with the impinging pump power P_{pump}, we have investigated the behavior of our tuneable OBS by detecting the fringe visibility ν versus P_{pump}. Measurements have been performed by applying a linear voltage to the piezomirror PM included in the interferometric part of the setup of Fig. 15. In this way, we were able to modify the optical path length of one of the two arms, thus allowing a scrolling of the fringe pattern on the PD and a measurement of I_{max} and I_{min} values, without shifting

the PD from the top of the impinging Gaussian beams. Indeed, a linear movement of the piezomirror in the direction normal to the mirror plane corresponds to a shift of the fringe pattern along a direction parallel to the PD surface; therefore, the output signal from the PD exhibits the sinusoidal behavior shown in Fig. 17.

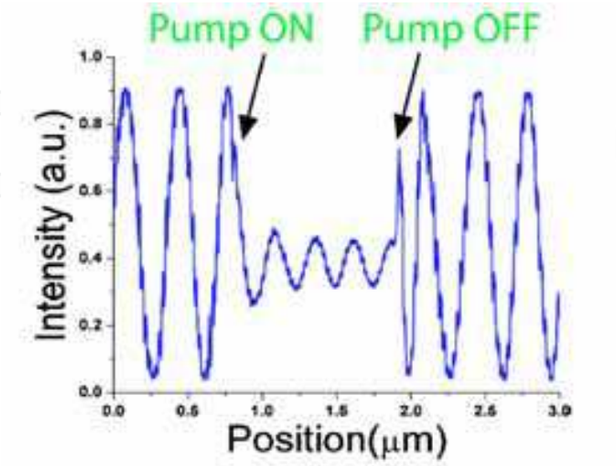

Fig. 17. Intensity profile of the interference pattern vs the piezomirror position. A reversible change of oscillation amplitude, obtained by switching ON and OFF the external pump can be well observed

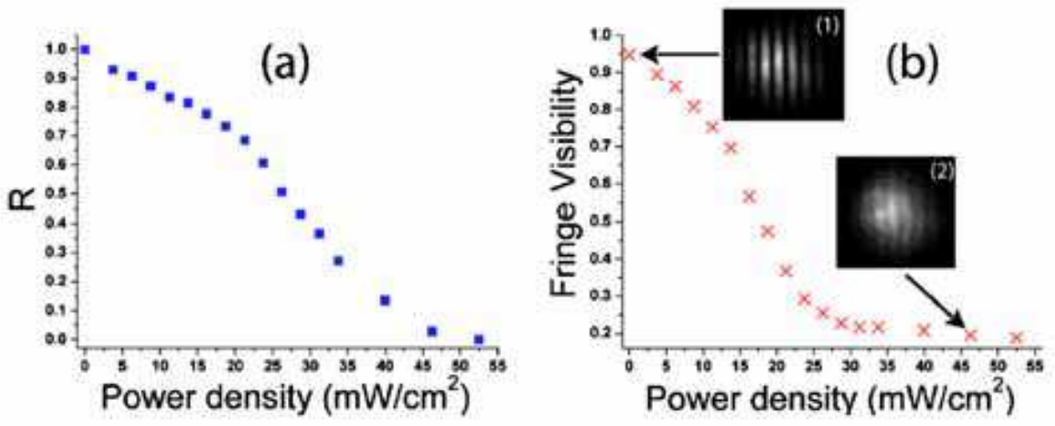

Fig. 18. Beam splitting (a) and fringe visibility (b) vs the pump power density. Interference pattern acquired with a CCD camera is reported for ν=0.94 (1) and ν=0.2 (2). Experimental errors are the order of dot and cross dimensions

The amplitude of the sinusoidal modulation is strongly attenuated when irradiating with a green pump laser (P_{pump}=48 mW/cm2) over the spot of the red light; oscillation amplitude is restored to its initial value in some milliseconds by turning off the external pump. The behavior of ν versus fine variations in P_{pump} is reported in Fig. 18b, along with measured values of R. Curves can be explained by considering that the rate of the trans–cis isomerization process depends on the number of excited molecules; therefore, the rate of concentration of photoisomerized azo-LC molecules is proportional to the pump power

density. This phenomenon directly affects R and therefore ν, which varies from 0.94 to 0.20. Fig. 18a shows that R values can be finely adjusted between 1 (transmitted and diffracted beams of the same intensity) and 0 (no diffracted beam, the whole impinging intensity is transmitted).
As for the measured ν values, following eq. (9), also ν should vary between 1 (when R=1) and 0 (when R=0). The observed discrepancy (0.92 instead of 1 and 0.2 instead of 0) can be explained by taking into account that, due to the birefringence of the grating [Caputo et al, 2010] the transmitted beam is elliptically polarized, with an ellipticity of the order of a/b≈10/1 where a and b are the major and minor axes of the polarization ellipse, respectively. The weak component polarized perpendicularly to the diffracted field is responsible for the small discrepancy between measured and predicted ν values.

5. The POLICRYPS as an array of optical resonators

A new intriguing scenario of applications emerges if we explore the possibility of obtaining a lasing action in POLICRYPS structures. Indeed, in recent years, many efforts have been spent in research for the realization of lasing devices based on organic systems: good candidate materials for achieving this result are cholesteric liquid crystals (CLCs). It is well known that CLC materials possess a helical periodic superstructure which provides a 1D spatial modulation of the refractive index [de Gennes, 1993]. This system behaves as a photonic band gap (PBG), i.e. it exhibits a window in the electromagnetic spectrum where wave propagation is forbidden. This is due to a mechanism known in literature as distributed feedback (DFB), and has the consequence that the system behaves as a mirrorless optical resonator. If the CLC material is doped with fluorescent guest molecules, a gain enhancement of the radiation, propagating in the structure, is possible. Kogelnik and Shank [Kogelnik & Shank, 1971] were the first to report laser action in mirrorless periodic Bragg DFB structures, while laser action in chiral liquid crystals was predicted by Goldberg and Schnur [Goldberg & Schnur, 1973]. There are many advantages in using POLICRYPS as a host structure for dye doped CLC helices. The sharp and parallel channels of POLICRYPS can behave as an array of optical resonators, each of them working as a microlaser. The length of the single channel is not limited by the sample geometry; in principle the single cavity can be several centimetres long, thus containing thousands of periods of the CLC helices. At the same time, its volume can be reduced at will by changing the periodicity of the structure. Optical resonators with these two features present a high quality factor Q and correspond to very efficient microcavity lasers. Such an array of microlasers has been experimentally realized in a POLICRYPS structure [Strangi et al, 2005]. A slightly different chemical mixture was used: a small amount (0.7 wt%) of Irgacure 2100 and Darocur 1173 photoinitiators (1:1 wt%, Ciba Specialty Chemicals) was used to reinforce the polymeric network and a 0.09 wt% of pyrromethene dye (Exciton) was added, which represented the gain medium of our system. Other components were 29.9 wt% BL088 cholesteric liquid crystal (Merck), and 69.3 wt% of NOA-61 monomer (Norland). The mixture was introduced by capillarity between ITO-coated glass plates separated by 13.5 μm thick mylar spacers. The sample was then prepared by following the typical recipe for obtaining POLICRYPS. The only difference is that the curing temperature was sensitively higher in order to bring the CLC material in the isotropic phase during curing. At the end of the whole process, an almost complete phase separation was obtained, giving rise to helixed liquid crystal

channels periodically separated by polymer walls. A scanning electron microscopy analysis of the sample showed a periodicity of 5 μm with the microcavity width of about 1.5 μm. The system was optically pumped with the second harmonic (λ = 532 nm) of a Nd:YAG laser. The laser beam was focused onto the sample by means of a cylindrical lens (f = 100 mm) and linearly polarized perpendicularly to the microchannels. The long axis of the section was oriented perpendicularly to the orientation of the polymeric walls; therefore, the profile obtained (long axis of approximately 5 mm) ensured the simultaneous excitation of multiple microchannels. Above a certain pump power, stimulated emission was achieved, emerging from the microcavities in a direction parallel to the glass plates and along the microchannels. At their end highly sensitive emission measurements were performed in a restricted cone angle of about 0.1 rad. The sketch in Fig. 19 shows this lasing scenario of the microlaser array.

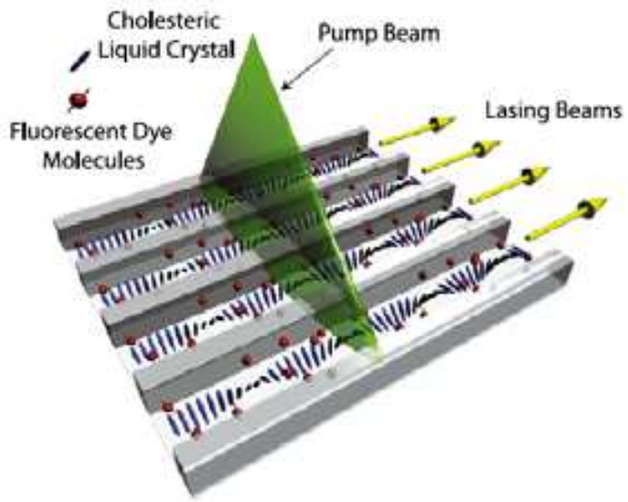

Fig. 19. Sketch of a multilaser array realized in a POLICRYPS structure

The stimulated emission emerging from the microchannels was circularly polarized, demonstrating that the distributed feedback mechanism due to the CLC helices is the cause of the observed phenomenon. The dependence of the emitted intensity and spectral linewidth (FWHM) on the input pump energy are reported in Fig. 20.

At low excitation energies, both the emission intensity and the linewidth show a quasilinear dependence on the pump energy. Above a characteristic threshold (the pump energy per excited sample area was about 5 mJ/cm^2, which corresponds to about 25 nJ/pulse), the emitted intensity suddenly starts to increase nonlinearly. Also, above this threshold, the emission linewidth breaks off from the previous trend and begins to decrease significantly. The observed pump energy value at which the power explosion and line narrowing effects occur (25 nJ/pulse) is one order of magnitude lower than in the case of other conventional dye-doped systems in a similar environment and under the same pumping conditions.

A striking scenario is presented in Fig. 21, showing the spatial distribution of the laser emission emerging from the microcavity laser array. A high sensitivity and resolution (1390 × 1024 12-bit PixelFlyQe, PCO) imaging CCD camera was employed in order to check the near-field modal profile of the stimulated emission. Images were acquired by scanning in the proximity of the output edge of our sample cell, in a direction perpendicular to the

microchannels. The mapped intensity profile hereby obtained indicates that the maxima of lasing intensities have a spatial recurrence, with a periodicity that is found to be about 5 μm; this value is in perfect agreement with the initial tailoring configuration (i.e. the distance between the polymeric walls).

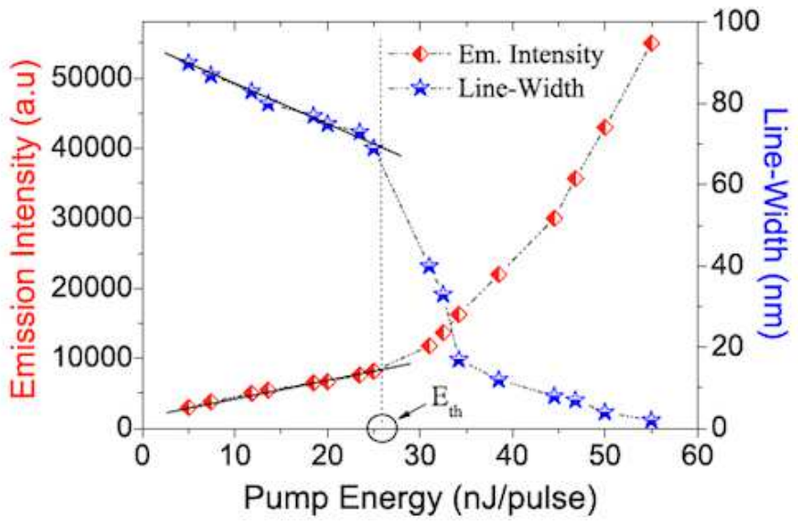

Fig. 20. Emitted intensity and linewidth dependence on input pump energy. Above a threshold of 25 nJ/pulse the reported curves change from initial regimes while lasing occurs

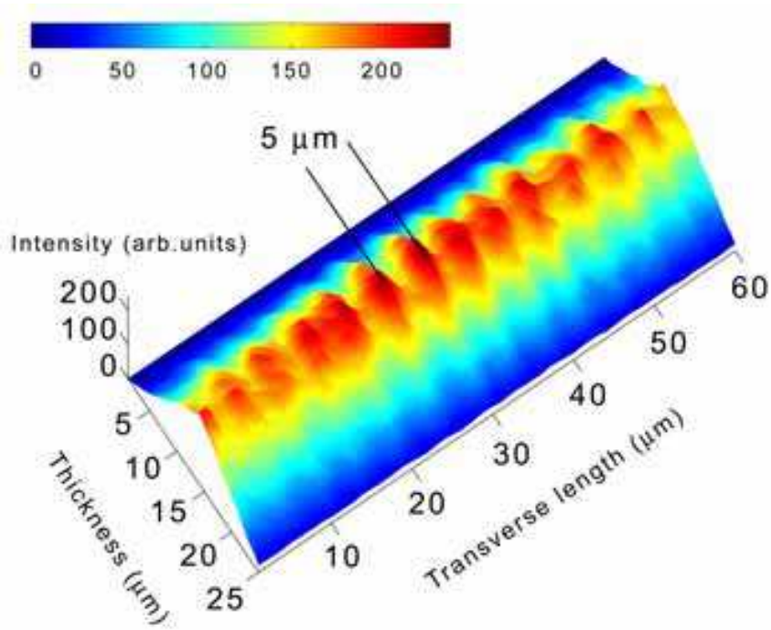

Fig. 21. Spatial distribution of the laser emission emerging from the mirrorless microcavity laser array. The periodicity of maximum intensities is 5 μm. This value is in agreement with the tailoring distance between the polymeric microchannels

Therefore we can definitely conclude that POLICRYPS microchannels act as miniaturized mirrorless cavity lasers, where the emitted laser light propagates along the liquid crystal helical axis, which behaves as a Bragg resonator.
This level of integration can lead to new photonic chip architectures and devices, such as a zero-threshold microlaser, phased array, discrete cavity solitons, filters, and routers. Furthermore, tailoring a proper array of electrodes, which enables the application of a local electric field, would give rise to electrically programmable phase holograms with interesting light polarization properties. Then, by including different dyes in neighbour channels, and by using proper microfibres connected at the exit, the result should be a multi-colour microlaser array with the possibility to control the intensity of each channel separately.

6. POLICRYPS with metallic nanoparticle inclusions

Noble metal nanoparticles (NPs) exhibiting plasmonic properties attract wide interest in research for the possibility they offer to realize metamaterials [Rockstuhl et al, 2007]. These have been predicted in 1969 by Veselago [Veselago, 1968] and they are materials that gain peculiar electromagnetic properties (e.g. negative refractive index) from their structure, rather than from their chemical composition. Thanks to recent advances in nanofabrication, first examples of such materials, which exhibit particular functionalities at optical frequencies, have been realized [Valentine et al, 2008]. However, the success of these results is limited by the typical size of devices that can be fabricated, which is actually very small (few square millimetres). Alternative approaches are emerging, which propose the use of self-assembling materials in order to overcome this issue and obtain the sought for greater structures, with less difficulty [Nanogold, (2009-2012; Metachem (2009-2013)]. An ambitious project is to combine metallic units with host materials whose dielectric properties can be tuned by an external control; indeed, a modification of the dielectric behavior of the host could correspond to a tuning action of the plasmon resonance frequency [Kossyrev et al, 2005]. In this regard, by combining the tunability of POLICRYPS structures with the plasmonic response of metallic NPs could give rise to novel metamaterial devices with tunable properties.

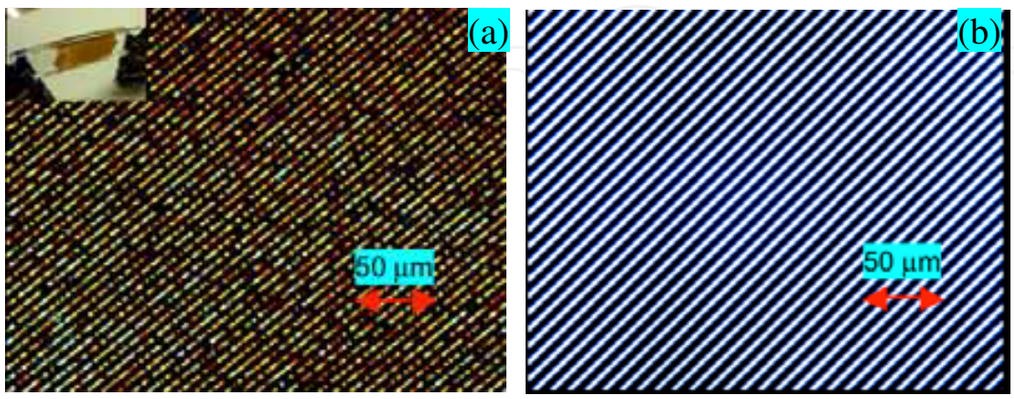

Fig. 22. Polarizing optical microscope images of (a) POLICRYPS diffraction grating with Ag NP inclusions; (b) typical POLICRYPS diffraction grating. In the inset of Fig.1a, a photograph which shows the brownish color of the realized new sample

In order to obtain a POLICRYPS structure that includes metallic NPs, we have used the Harima Silver nanopaste NPS-J (from Harima Chemicals, Inc.) that is generally involved with other applications (e.g. ink-jet printing and laser sintering) [Niizeki et al, 2008].
After some difficulties encountered for mixing this Harima material with the standard POLICRYPS precursor [Caputo et al, 2011b], we obtained a new mixture composed by: NOA61, 68.5 wt%; NPS-J, 3.5 wt%; E7, 28.0 wt%. The experiment followed the same procedure used for fabricating a standard POLICRYPS structure [Caputo, 2004]: the mixture has been sandwiched by capillarity in a 13μm thick glass cell and then, by keeping it at high temperature (about 70°C), it has been exposed to a UV interference pattern with a periodicity of 6μm. A microphotograph of the fabricated sample, observed between crossed polarizers at the polarizing optical microscope (POM), is reported in Fig. 22a along with the picture of a typical POLICRYPS structure without NPs (Fig. 22b) reported for comparison aims. Some morphological differences between the two structures are evident which are obviously due to the presence of metal nano-particles in the new sample.
A SEM micrograph of the same sample (Fig. 23) reveals that the NPs are organized in clusters (the typical size ranging between 0.3μm and 1μm), homogeneously distributed all over the grating area, and visible as bright spots. Of course, those clusters that are trapped in the LC films locally disturb the order of the nematic director but, nevertheless, large LC domains, with the director aligned perpendicularly to the polymer slices of the structure, are still present. This feature, which is typical of a standard POLICRYPS grating, is evident by rotating the sample between crossed polarizers.

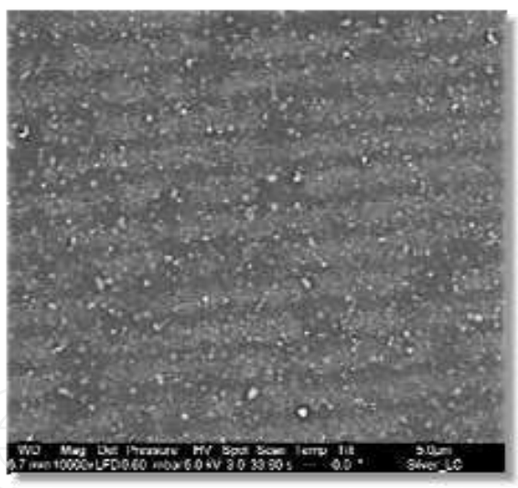

Fig. 23. scanning electron microscope image of the POLICRYPS diffraction grating with Ag NP inclusions; Ag clusters (with size ranging between 0.3μm and 1μm) are visible in the picture as bright spots

6.1 Spectroscopical characterization

As a consequence of considerations in paragraph 3.2, if we illuminate a POLICRYPS structure (not including metallic NPs) with linearly polarized white light (wavelength in the range 350-1100nm, at normal incidence), we expect a behaviour that is strongly dependent on the incident polarization state. In particular, we can expect that the polarization parallel to the nematic director **n** (p-type) is diffracted by the grating and hence the light

transmission is almost suppressed. On the other hand, the orthogonal polarization (s-type) is, instead, highly transmitted in the whole analyzed range (350-1100nm), because the experienced refractive index modulation is limited and the grating is almost absent. By repeating the same experiment with the NP doped POLICRYPS sample, new features come out. As in the case of a standard POLICRYPS, the p-polarized light is diffracted by the structure and the transmission of the grating is negligible for almost all the visible part of the spectrum (Fig. 24, GPP curve). For the orthogonal polarization (s-type), we observe instead a highly transmitted intensity, whose spectrum exhibits a peculiar behaviour (Fig. 24, curve GSP). The polarization sensitivity of the grating is further on demonstrated by the GNP curve reported in the middle of Fig. 24, obtained by probing the grating with unpolarized light: the behaviour of this spectrum represents a kind of "average" of the two, differently polarized, ones. A comparison of the GSP curve (Fig. 25, top curve) with the spectrum transmitted by a mixture of Harima NPs dissolved in Chloroform (Fig. 25, bottom curve) can help to interpret above results. Indeed, the shape of this curve has particular features, exhibiting a transmission minimum at λ≈520nm. The typical plasmonic response of Harima NPs (20-50nm in diameter) is peaked around λ=400nm; in presence of Ag clusters (0.3-1μm), not perfectly diluted in Chloroform, we can expect a shift of the Ag plasmonic resonance to the observed value [Mock et al, 2002]. A similar minimum, can also be noted in the GSP curve (500÷570nm) of the NP doped POLICRYPS sample. Given that the grating is almost absent for the s-polarized light (the diffraction pattern can hardly be seen in this condition), our guess is that the shape of the GSP curve of Fig. 24 reveals the presence of Ag clusters within the structure.

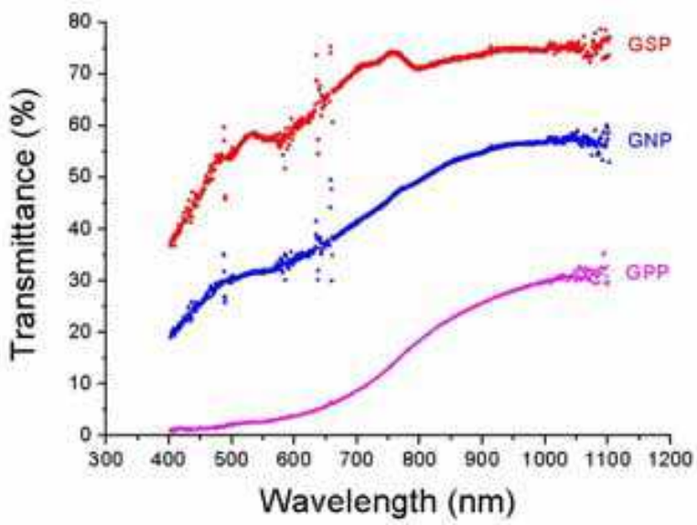

Fig. 24. Spectral response of the newly realized POLICRYPS structure containing Ag NPs. Top and bottom curves have been obtained by probing the sample with s-polarized light (GSP) or p-polarized light (GPP) respectively; In the middle, the curve obtained by probing the grating with unpolarized light (GNP)

Above considerations can just give a qualitative proof of that guess and, as such, further investigations are essential in order to provide a quantitative confirmation. However, in case of a positive outcome, these novel structures could reveal quite promising for the realization of polarization sensitive plasmonic devices.

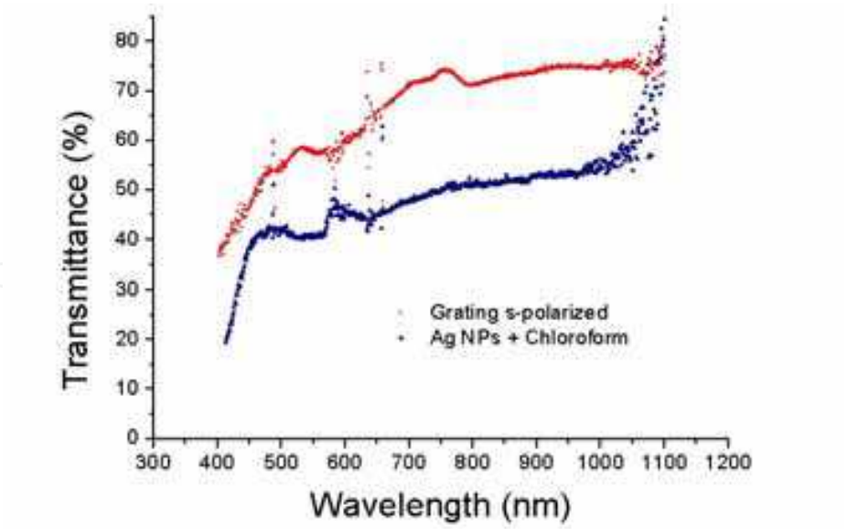

Fig. 25. Comparison between the spectral response of pure Ag NPs in Chloroform (bottom curve, 5x factor) and that of Ag NPs inclusions in a POLICRYPS structure (top curve, sample probed with s-polarized white light)

7. Conclusion

In the field of electrically switchable devices, exploiting liquid crystalline composite materials, POLICRYPS represents a very promising nano/microstructure with several possibilities of application. Indeed, few main features of this system act as a common denominator for these applications: the sharpness of the structure and the uniformity of the LC films minimize light scattering losses, while the application of a suitable, relatively low, external voltage can determine, in a millisecond timescale, a reorientation of the LC director and hence the tunability of the device. Depending on the way a light beam propagates through, the POLICRYPS can be used as a switchable diffraction phase grating, for light impinging at a given angle with the structure; a switchable optical phase modulator (with a light beam impinging almost perpendicularly to the structure); an all-optical switchable device, an array of mirrorless optical micro-resonators devoted to obtain a tuneable lasing effect (if the NLC is substituted with a mixture of dye-doped CLC and the system is optically pumped) and a plasmonic device with polarization sensitive properties (when metallic nanoparticles are included in the chemical mixture). Performances exhibited in all the above applications are very interesting and stimulate further investigations in the different fields.

8. Acknowledgment

Our sincere thanks go to Dr. Giuseppe Strangi and his group for the fruitful collaboration in the realization and characterization of microlaser arrays in POLICRYPS structures and to Dr. Nelson Tabiryan and his group for the possibility offered in realizing Azo-materials doped POLICRYPS structures.
Finally, the research leading to these results has received funding from the European Union's Seven Framework Programme (FP7/2007-2013) under grant agreement n°228455.

9. References

Bunning, T.J.; Natarajan, L.V.; Tondiglia, V.P. & Sutherland, R.L. (2000). *Holographic polymer-dispersed liquid crystals (H-PDLCs)*, Annu. Rev. Mater. Sci. Vol. 30, pp. 83-115

Caputo, R.; Sukhov, A.V.; Umeton, C.P. & Ushakov, R.F. (2000). *Formation of a grating of submicron nematic layers by photopolymerization of nematic-containing mixture*, J. Exp. Theor. Phys. Vol. 91 pp. 1190–1197

Caputo, R.; Sukhov, A.V.; Tabyrian, N.V.; Umeton, C.P. & Ushakov, R.F. (2001). *Mass transfer processes induced by inhomogeneous photo-polymerisation in a multicomponent medium*, Chem. Phys. Vol. 271, pp. 323–335

Caputo, R.; De Sio, L.; Sukhov, A.V.; Veltri, A. & Umeton, C.P. (2004). *Development of a new kind of switchable holographic grating made of liquid crystal films separated by slices of polymeric material (policryps)*, Opt. Lett. Vol. 29, pp. 1261-1263

Caputo, R.; Umeton, C.P.; Veltri, A.; Sukhov, A.V. & Tabiryan, N. (2007). *Holographic diffraction grating,process for its preparation and opto-electronic devices incorporating it*, European Patent Request 1649318; US Patent Request 2007/0019152A1

Caputo, R.; Trebisacce, I.; De Sio, L. & Umeton, C.P. (2010). *Jones matrix analysis of dichroic phase retarders realized in soft matter composite materials*, Opt. Express Vol. 18, pp. 5776-5784

Caputo, R.; Trebisacce, I.; De Sio, L. & Umeton, C.P. (2011a). *Phase modulator behavior of a wedge-shaped POLICRYPS diffraction grating*, Mol. Cryst. Liq. Cryst. (accepted)

Caputo, R.; De Sio, L.; Dintinger, J.; Sellame, H.; Scharf, T. & Umeton, C.P. (2011b). *Realization and characterization of POLICRYPS-like structures including metallic subentities*, Mol. Cryst. Liq. Cryst. (submitted)

de Gennes, P.G. (1993). *The Physics of Liquid Crystals* (Oxford: Clarendon)

De Sio, L.; Caputo, R.; De Luca, A.; Veltri, A.; Sukhov, A.V. & Umeton, C.P. (2006). *In situ optical control and stabilization of the curing process of policryps gratings*, Appl. Opt. Vol. 45, pp. 3721-3727

De Sio, L.; Veltri, A.; Tedesco, A.; Caputo, R.; Sukhov, A.V. & Umeton C.P. (2008a). *Characterization of an active control system for holographic set-up stabilization*, Appl. Opt. Vol. 47, pp. 1363-1367

De Sio, L.; Tabiryan, N.; Caputo, R.; Veltri, A. & Umeton C.P. (2008b). *Policryps structures as switchable optical phase modulators*, Opt. Express Vol. 16, pp. 7619–7624

De Sio, L.; Serak, S.; Tabiryan, N.; Ferjani, S.; Veltri, A. & C. Umeton, (2010). *Holographic Gratings Containing Light-Responsive Liquid Crystals for Visible Bichromatic Switching*, Adv. Mater. Vol. 22, pp. 2316-2319.

EU Project: "Self-organised nanomaterials for tailored optical and electrical properties (Nanogold)", FP7-NMP-SMALL-2008-228455, nanogold.epfl.ch, (2009-2012); EU Project: "Nanochemistry and self-assembly routes to metamaterials for visible light (Metachem)", FP7-NMP-SMALL-2009-228762, www.metachem-fp7.eu, (2009-2013).

Goldberg, L.S. & Schnur, J.M. (1973). *Tunable internal-feedback liquid crystal laser*, US Patent Specification 3 771 065

Kogelnik, H. (1969). *Coupled Wave Theory for Thick Hologram Gratings*, Bell Syst. Tech. J. Vol. 48, pp. 2909-2948

Kogelnik, H. & Shank, C.V. (1971). *Stimulated emission in a periodic structure*, Appl. Phys. Lett. Vol. 18, pp. 152-154

Kossyrev, P.A.; Yin, A.; Cloutier, S.G., Cardimona, D.A.; Huang, D.; Alsing, P.M. & Xu, J.M.; (2005) *Electric Field Tuning of Plasmonic Response of Nanodot Array in Liquid Crystal Matrix*, Nano. Lett. Vol. 5, pp. 1978-1981.

Lucchetta, D.E.; Criante, L. & Simoni, F. (2003) *Optical characterization of polymer dispersed liquid crystals for holographic recording*, J. Appl. Phys. Vol. 93, pp. 9669-9675

Margerum J.D.; Lackner, A.M.; Ramos, E.; Smith, G.W.; Vaz, N.A.; Kohler, J.L. & Allison, C.R. (1992). *Polymer dispersed liquid crystal film devices*, US Patent Specification 5,096,282, March 17, 1992

Mock, J.J.; Barbic, M.; Smith, D.R.; Schultz, D.A. & Schultz, S. (2002). *Shape effects in plasmon resonance of individual colloidal silver nanoparticles*, J. Chem. Phys. Vol. 116, 6755-6759

Niizeki, T.; Maekawa, K.; Mita, M.; Yamasaki, K.; Matsuba, Y.; Terada, N. & Saito, H.; (2008) *Laser Sintering of Ag Nanopaste Film and Its Application to Bond-Pad Formation*, Proc. ECTC 2008.

Ozaki, M.; Kasano, M.; Ganzke, D.; Haase, W. & Yoshino, K. (2002) *Mirrorless lasing in a dye-doped ferroelectric liquid crystal*, Adv. Mater. Vol. 14, pp. 306-309

Rockstuhl, C.; Lederer, F.; Etrich, C.; Pertsch, T & Scharf, T.; (2007). *Design of an Artificial Three-Dimensional Composite Metamaterial with Magnetic Resonances in the Visible Range of the Electromagnetic Spectrum*, Phys. Rev. Lett. Vol. 99, 017401.

Strangi, G.; Barna, V.; Caputo, R.; De Luca, A.; Versace, C.; Scaramuzza, N.; Umeton, C.P. & Bartolino, R. (2005) *Color-tunable organic microcavity laser array using distributed feedback*, Phys. Rev. Lett. Vol. 94, 063903

Sutherland, R.L.; Tondiglia, V.P.; Natarajan, L.V.; Bunning, T.J. & Adams W.W. (1994). *Electrically switchable volume gratings in polymer-dispersed liquid crystals*, Appl. Phys. Lett., Vol. 64, pp. 1074–1076

Sutherland R.L., Tondiglia V.P., Natarajan L.V., Bunning T.J. & Adams W.W. (1996). *Electro-optical switching characteristics of volume holograms in polymer dispersed liquid crystals*, J. Nonlinear Opt. Phys. Mater., Vol. 5, pp. 89–98

Tsutsumi, O. & Ikeda, T.; (1995). *Optical switching and image storage by means of azobenzene liquid-crystal films*, Science Vol. 268, pp. 1873-1875

Yariv, A. (1989). *Quantum Electronics* (Wiley, New York)

Valentine, J.; Zhang, S.; Zentgraf, T.; Ulin-Avila, E.; Genov, D.A.; Bartal, G. & Zhang, X.; (2008). *Three Dimensional Optical Metamaterial Exhibiting Negative Refractive Index*, Nature, vol. 455, 376.

Veselago, V.G.; (1968). *The electrodynamics of substances with simultaneously negative values of* ε *and* μ, Sov. Phys. Usp, Vol. 10, 4, 509-514 (1968).

Wu, Y.H.; Lin, Y.H.; Lu, Y.Q.; Ren, H.; Fan, Y.H.; Wu, J. & Wu, S.T. (2004). *Submillisecond response variable optical attenuator based on sheared polymer network liquid crystal*, Opt. Express Vol. 12, pp. 6382–6389

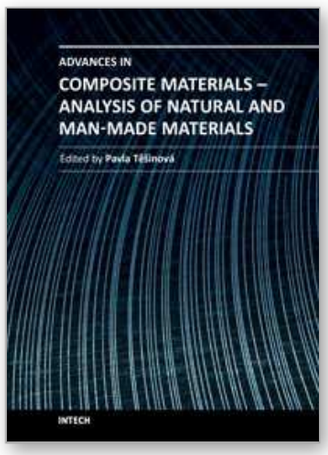

Advances in Composite Materials - Analysis of Natural and Man-Made Materials

Edited by Dr. Pavla Tesinova

ISBN 978-953-307-449-8
Hard cover, 572 pages
Publisher InTech
Published online 09, September, 2011
Published in print edition September, 2011

Composites are made up of constituent materials with high engineering potential. This potential is wide as wide is the variation of materials and structure constructions when new updates are invented every day. Technological advances in composite field are included in the equipment surrounding us daily; our lives are becoming safer, hand in hand with economical and ecological advantages. This book collects original studies concerning composite materials, their properties and testing from various points of view. Chapters are divided into groups according to their main aim. Material properties are described in innovative way either for standard components as glass, epoxy, carbon, etc. or biomaterials and natural sources materials as ramie, bone, wood, etc. Manufacturing processes are represented by moulding methods; lamination process includes monitoring during process. Innovative testing procedures are described in electrochemistry, pulse velocity, fracture toughness in macro-micro mechanical behaviour and more.

INTECH
open science | open minds

InTech Europe
University Campus STeP Ri
Slavka Krautzeka 83/A
51000 Rijeka, Croatia
Phone: +385 (51) 770 447
Fax: +385 (51) 686 166
www.intechopen.com

InTech China
Unit 405, Office Block, Hotel Equatorial Shanghai
No.65, Yan An Road (West), Shanghai, 200040, China
中国上海市延安西路65号上海国际贵都大饭店办公楼405单元
Phone: +86-21-62489820
Fax: +86-21-62489821

IntechOpen